ELECTRONICS AND ELECTRICAL ENGINEERING
ISSN 1392 – 1215 2012. No. 2(118)
ELEKTRONIKA IR ELEKTROTECHNIKA

ELECTRICAL ENGINEERING
T 190
ELEKTROS INŽINERIJA

Power Factor Correction based on Fuzzy Logic Controller with Fixed Switching Frequency

A. Kessal, L. Rahmani, M. Mostefai
Laboratoire d'Automatique (LAS), Université Ferhat Abbas, Faculté de Technologie, Département d'électrotechnique, Sétif, Algeria.phone : +213790721151, e-mail: k_maintenance@yahoo.fr
J. Gaubert
Laboratoire d'Automatique et d'Informatique Industrielle (LAII), ESIP, Université de Poitiers, France

crossref http://dx.doi.org/10.5755/j01.eee.118.2.1176

Introduction

Single-phase power factor correction (PFC) circuits provide rectification of the line voltage to a regulated dc voltage while shaping the input current to be a sinusoid and in phase with the line voltage [1]. Often, the PFC acts as a pre-regulator to a dc–dc converter that may be used to provide additional regulation and ohmic isolation [2]. Due to adoption of IEC 1000-3-2 as the EN61000-3-2 norm in Europe and the formulation of the IEEE 519 [3] in USA, these circuits are increasingly being used in the front-end of electronic equipments. Among the several possible topologies[2], the boost PFC shown in Fig. 1 is most commonly used. The control objectives are to track the inductor current to a rectified Sinusoid (the line current is sinusoidal and in phase with the line voltage) and to regulate the average output voltage to desired magnitude with fast response to the load variation [4].

Recent research has been directed at applying nonlinear control principles to the dynamic control of converters. The system is controlled by fuzzy control algorithm, in which a set of linguistic rules written in accordance to experience and intuitive reasoning. However, if the control methodology is directly applied to classical ac-dc converters with APFC [5], it might impose considerable computation time to deal with the fast-varying current loop. Fuzzy logic control has been investigated for applications such as motor drives and dc-dc converters [6]. Objectives include tight output voltage regulation, high rejection of reference output voltage variations and load transients. The improvement in the transient response of the controller voltage loop decreases the quality of the input current (High THD). On the other hand, PI controller design in current loop requires an accurate mathematical model of the plant and it failed to perform satisfactorily under parameter variation, nonlinearity (two multiplications), load disturbance, etc [7]. Hysteresis current controller (bang-bang hysteresis (BBH) technique) has an advantage in coping with the time varying nonlinearity of switches in PFC pre-regulator, and it does not require an accurate mathematical model of the PFC pre-regulator when the controller is being designed [8]. Also this technique has an advantage of yielding instantaneous current control, which results in very fast response and increased switch reliability. However, it has a serious disadvantage in that the switching frequency of the boost switch f_{sw} is not constant and varies in a wide range during each half cycle of the ac input voltage [9]. The switching frequency is also sensitive to circuit component values, design parameters and difficult for EMI filter design. The novel feature of the proposed method resides in the fact that unity power factor and nearly sinusoidal input current are obtained at constant switching frequencies [10]. Moreover, the method exhibits an instantaneous control of current, which results in very fast response and increased switch reliability.

This paper presents a systematic design, digital implementation and experimental comparison, in first a PI and fuzzy logic controllers with a 100Hz notch filter for a voltage loop of the regulated dc voltage, then the standard hysteresis controller and redesign with some modifications for improved performance in the current loop. All these controllers are verified by detailed MATLAB/Simulink based simulations through the use of a continuous time plant model and a discrete time controller. Design is comprehensive in the sense that it accounts for sampling effects, computation delays, hardware filtering for antialiasing and software filtering for measurement noise reduction. Real-time implementation is done on an experimental test bench using the dSPACE DS1104 controller board. These controllers are experimentally compared for steady-state performance and transient response over the entire range of input and load conditions for which the system is designed.

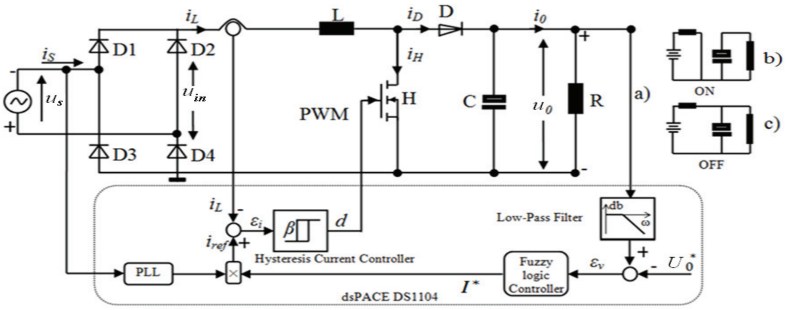

Fig. 1. APFC pre-regulator

Voltage-loop controller

PI-Controller. As shown in Fig. 2, the dc-bus voltage u_0 is sensed and compared with a reference value U_0^*. The obtained error is used as input for the PI controller, the output of the controller I^* multiplied by $|\sin\omega t|$ obtained from PLL stage with sensing of the input voltage is the instantaneous reference current command i_{ref}.

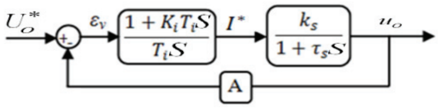

Fig. 2. PI-Controller for APFC

$\frac{1+K_iT_is}{T_is}$ is the transfer function of the PI-Controller; $K_i=\frac{RC}{2T_i}$, $T_i=\frac{ARU_{\text{SM}}}{8\pi f_{\text{CV}}U_0^*}$: are the PI parameters; f_{CV} is the voltage closed loop crossover frequency.

The system in Fig. 1 is modeled as a first order system

$$\frac{u_0}{I^*}=\frac{U_{SM}}{4U_0^*}\frac{R}{1+\frac{RC}{2}s}=\frac{k_s}{1+\tau_s s}. \tag{1}$$

Pole and gain are chosen to obtain a sufficient phase margin gain (*≈45°*) and bandwidth in the 5Hz to 20Hz range. The bandwidth is intentionally kept very low since the compensator gain at 100Hz effectively determines the third harmonic to be expected in the input current. Since the outer loop has a finite dc gain, the voltage reference is pre-compensated to avoid a steady state voltage error at nominal operation. With f_{CV}=10Hz, K_{i}=2.0160 and T_{i}=0.0494, the closed loop transfer function with the design example given in table 1 is

$$\frac{u_0}{U_0^*}=\frac{k_{\text{F}}}{1+\tau_{\text{F}}s}=\frac{16}{1+0,0159s}\ , \tag{2}$$

The circuit is designed with the following specification (Table 1).

Fuzzy Logic-Controller. The fuzzy logic controller unlike conventional controllers does not require a mathematical model of the system that should be controlled. However, a comprehending of the system and the control requirements is necessary. The fuzzy controller designer must clarify how the information is processed (control strategy and decision), and information flows out of the system (solution/output variable). The fuzzy logic controller consists of three basic blocks: Fuzzification; Inference Mechanism and Defuzzification

Table 1. Design specification and circuit parameters

Desired switching frequency	f_{swd}=20kHz
Output power	P_0=121W
Magnitude of supply voltage	U_{SM}=150V
DC-Bus reference output voltage	U^*_0=160V
Input current ripple	≤2,5%
Output voltage ripple	≤2%
Load resistance	R=212Ω
Input Inductance	L=22,5mH
Output Capacity	C=940µF

Fig. 3. shows the block diagram of the proposed fuzzy logic control scheme of the boost rectifier with APFC. The dc-bus voltage v_0 is scaled and is sampled by the digital apparatus and compared with a reference value U_0^*. The obtained error $\varepsilon_{\text{v}}(k)=U_0^*(k)-u_0(k)$ and its incremental variation $C\varepsilon_{\text{v}}(k)=\varepsilon_{\text{v}}(k)-\varepsilon_{\text{v}}(k-1)$ at the k_{th} sampling instant are used as inputs of fuzzy controller. The output is the variation magnitude of reference current δI^*. The dc-bus voltage is controlled by adjusting the magnitude of reference current I^*. Where ρ and σ are constants used to normalize the error and the change of error.

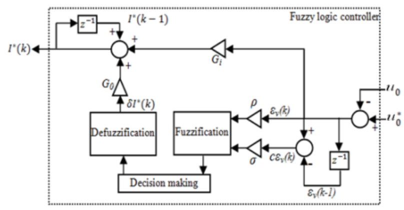

Fig. 3. Fuzzy logic-Controller for APFC

Table 2. Fuzzy control rules

		(ε_v)						
		NB	NM	NS	ZE	PS	PM	PB
($C\varepsilon_v$)	NB	NB	NB	NB	NB	NM	NS	ZE
	NM	NB	NB	NB	NM	NS	ZE	PS
	NS	NB	NB	NM	NS	ZE	PS	PM
	ZE	NB	NM	NS	ZE	PS	PM	PB
	PS	NM	NS	ZE	PS	PM	PB	PB
	PM	NS	ZE	PS	PM	PB	PB	PB
	PB	ZE	PS	PM	PB	PB	PB	PB

Current-loop controller

The PFC circuit analyzed here has a feedback loop such that the switching mode is determined by comparison of the actual current and sinusoidal reference current supplied form voltage loop controller in both ways the actual current oscillates in fixed band hysteresis (FBH) as shown in Fig.4. In the second way, the actual current oscillates in variable band hysteresis (VBH).

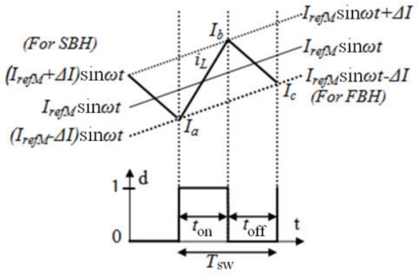

Fig. 4. Switching frequency

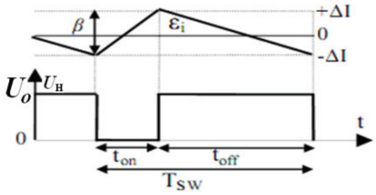

Fig. 5. Current error and the switch H voltage

Conventional Hysteresis Current Control. In this scheme, the algorithm is given as:

$$\text{Upper band}(i_{\text{upper}}) = I_{\text{refM}}\sin(\omega t) + \Delta I = I_{\text{refM}}\sin(\omega t) + \left(\frac{\beta}{2}\right), \tag{3}$$

$$\text{Lower band}(i_{\text{lower}}) = I_{\text{refM}}\sin(\omega t) - \Delta I = I_{\text{refM}}\sin(\omega t) + \left(\frac{\beta}{2}\right), \tag{4}$$

$$\text{If } i_{\text{L}} > i_{\text{upper}},\ d = 0,\ \text{then } u_{\text{H}} = U_0\ , \tag{5}$$

$$\text{If } i_{\text{L}} < i_{\text{lower}},\ d = 1,\ \text{then } u_{\text{H}} = 0\ , \tag{6}$$

where $\beta=2\Delta I$ is band hysteresis.

From Fig. 4 and Fig. 5 by considering the output voltage u_0 constant (U_0) over a switching period we can write:

$$t_{\text{on}} = \frac{L}{u_{\text{in}}}(I_b - I_a), t_{\text{off}} = \frac{L}{u_{\text{in}} - U_0}(I_c - I_b), \tag{7}$$

$$f_{\text{sw}} = \frac{1}{T_{\text{SW}}} = \frac{1}{t_{\text{on}} + t_{\text{off}}}. \tag{8}$$

From Fig.1, u_H is given

$$u_{\text{in}} - L\frac{di_{\text{L}}}{dt} = u_{\text{H}}. \tag{9}$$

For the ideal PFC, we assume i_{L} to the reference rectifier sinusoidal shape i_{ref}, the equation (9) becomes

$$u_{\text{in}} - L\frac{di_{\text{ref}}}{dt} = u_{\text{H}}^*. \tag{10}$$

From (9) and (10)

$$\frac{d\varepsilon_i}{dt} = u_{\text{H}} - u_{\text{H}}^*, \tag{11}$$

where $\varepsilon_{\text{L}} = i_{\text{ref}} - i_{\text{L}}$ – the error current in hysteresis band, u_H^* – the interrupter reference voltage.

From (11), if we assume the quantity $u_{\text{H}} - u_{\text{H}}^*$ constant during the switching period, then the error current $\varepsilon_i(t)$ varied as triangular form as shown in Fig. 5.

From Fig. 6 and (11), become t_{on} and t_{off}:

$$t_{\text{on}} = \frac{L\beta}{v_{\text{H}}^*}, t_{\text{off}} = \frac{L\beta}{U_0 - u_{\text{H}}^*}, \tag{12}$$

$$f_{\text{sw}} = \frac{u_{\text{H}}^*(U_0 - u_{\text{H}}^*)}{L\beta U_0}. \tag{13}$$

From (11) and (13), switching frequency is

$$f_{\text{sw}} = \frac{(u_{\text{in}} - L\omega i_{\text{ref}})(U_0 - u_{\text{in}} + L\omega i_{\text{ref}})}{LU_0\beta}, \tag{14}$$

where $u_{\text{in}} = U_{\text{SM}}|\sin(\omega t)|$, $i_{\text{ref}} = I_{\text{refM}}|\sin(\omega t)|$.

To investigate the control characteristics of a PFC, the variation of maximal switching frequency (MSF) with the inductance L of ΔI parameter for FBH is evaluated in Fig. 6.

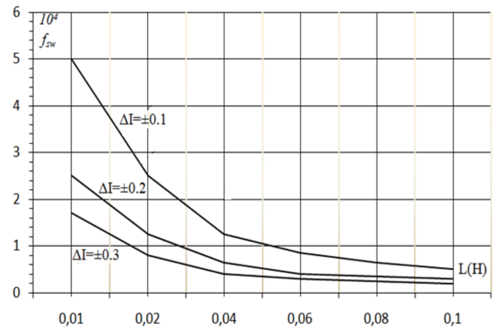

Fig. 6. Variation of switching frequency with L

The charts of $(f_{\text{sw}})_{\text{MAX}} = f(L)$ of parameter ΔI for FBH, informs us about the value of L to choose to limit the excursion in frequency to a compatible value. With 0,1H, the MSF is about 5 kHz. This relatively low frequency shows well the control by hysteresis. A more realistic simulation with L=0,0225H and thus an MSF of 20 kHz would allow faster variations of current i_{L} around his reference current i_{ref}.

Hysteresis current control with constant switching frequency. From (14), if β is constant and the time t varies, then the switching frequency f_{sw} also varies. To get f_{sw} constant, the hysteresis band has to be dynamically changes, according (15)

$$\beta = \frac{(u_{\text{in}} - L\omega i_{\text{ref}})(U_0 - u_{\text{in}} + L\omega i_{\text{ref}})}{LU_0 f_{\text{swd}}}, \tag{15}$$

where f_{swd} is the desired switching frequency. (15) gives a very simple control law with constant switching frequency allowing the improvement of characteristics of hysteresis current controller in terms of switching loss, audible noise and EME related problems.

Simulation and experimental results

Steady-state performance. Fig. 7 illustrate dc-bus voltage, line voltage, line current and his associated spectrum, for the Fuzzy_Hysteresis control with FBH and VBH, respectively at nominal load and nominal line voltage. From these figures, it can be seen that the results obtained with the proposed Fuzzy_Hysteresis control are much better than the international norms. Line current is very close to sine wave and in phase with the power source voltage, the THD is less than 4%. It is important to note that at nominal line and load condition, the Fuzzy_Hysteresis control with variable band hysteresis has THD number about 2,01% even with the limited bandwidth that is allowed by the digital implementation. With the variable band hysteresis control, THD of the input current is match better than with the fixed band hysteresis control; the steady-state error is 1V.

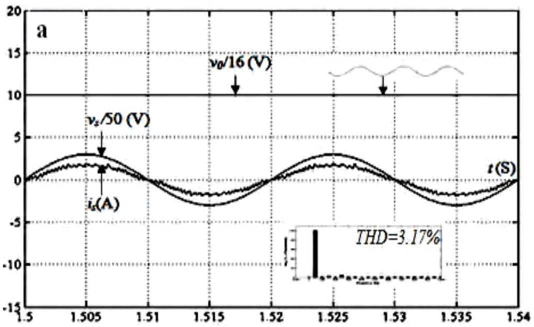

a)

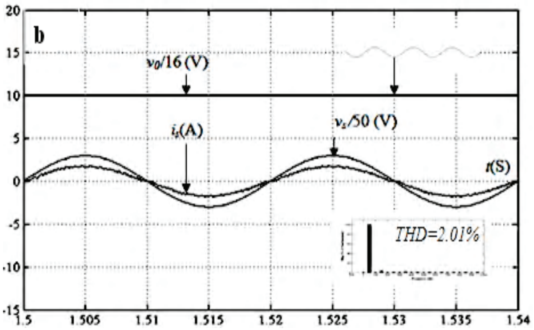

b)

Fig. 7. Simulated waveforms: a) using FBH, b) using VBH

Transient performance. As previously stated, step load changes are effected by connecting (or disconnecting) parallel load. The reference current amplitude is limited to 3,5A in the control for the Fuzzy and PI control designs. When the system has been entered into steady state, there is large step change in the load R from 212Ω to 312Ω with constant reference output voltage. The waveforms of the input current and the output voltage during transient period are shown in Fig. 9. After a short transient, the dc-bus voltage is maintained close to its reference value with a good approximation and stability. Afterwards, the load resistance is switched back to 212 Ω.

Another test on large-signal change of U_0^* has been performed, U_0^* is changed from 160V to 192V with *R* unchanged. The transient output voltage and the input current are shown in Fig. 10. The output voltage reached to the new value after 400ms. On the other hand, it can be observed that the input current is maintained in sinusoidal waveform during the transient period. When the system becomes stable, U_0^* is returned to 160V again. The settling time is about 400ms for the output voltage to attain the old value. Nevertheless, the input current is still sinusoidal and in phase with the input voltage during transient. It can be seen from the above that the system is stable during the large-signal change in the reference output voltage and the output load. Further research will be dedicated into the optimization of the fuzzy rules, in order to have further improvement in the transient behaviors.

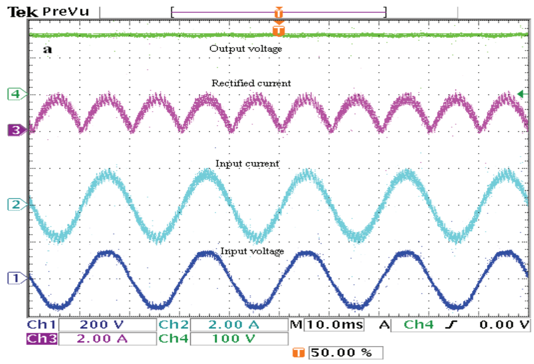

a)

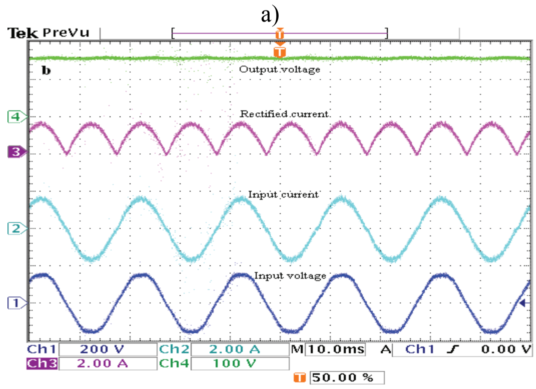

b)

Fig. 8. Steady state waveforms: a) with FBH, b) with VBH

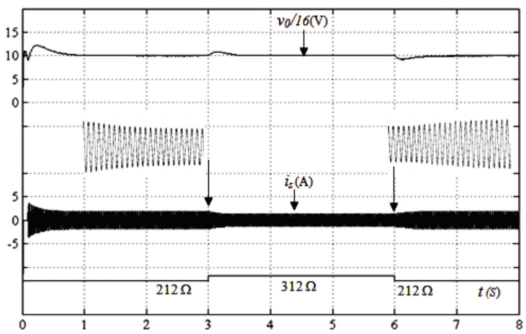

Fig. 9. Output voltage, input current (load changes)

Fig. 11 show experimental results for PI and fuzzy logic controller respectively of a step response against the disturbance load under the unity power factor operation. It can be observed from these results that the unity power factor operation is successfully achieved, *PF*=0,997, the reactive power is approximately equal to zero (0,3VAR) and the *DPF*=1 (*DPF* displacement power factor) even in this transient state. Notice that, after a short transient, the dc-bus voltage is maintained close to their reference values.

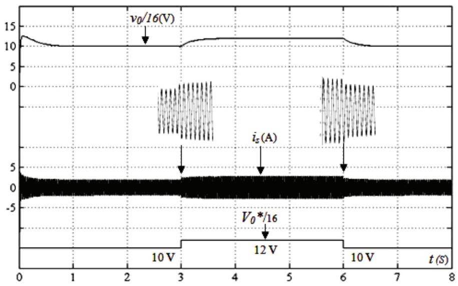

Fig. 10. Output voltage, input current (reference changes)

Fig. 12 show experimental results for PI and fuzzy logic controller respectively of a step response against the step change of U_0^*. Notice that, after a short transient, the dc-bus voltage is maintained close to their new reference values.

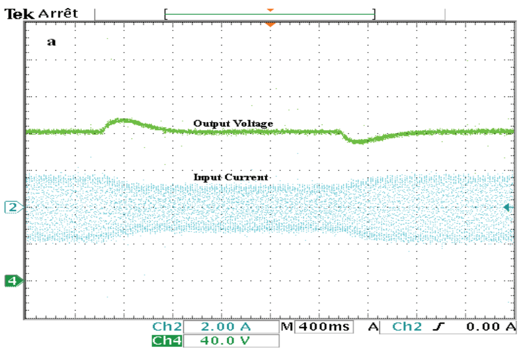

a)

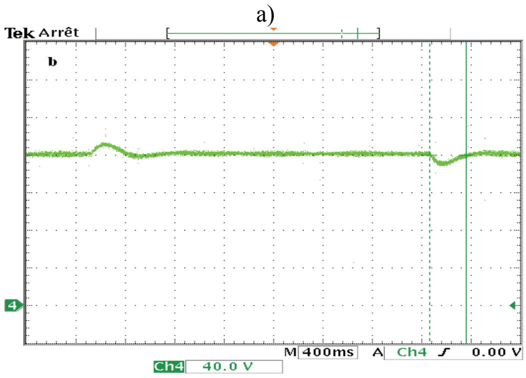

b)

Fig. 11. Transient load changes: a) PI, b) Fuzzy

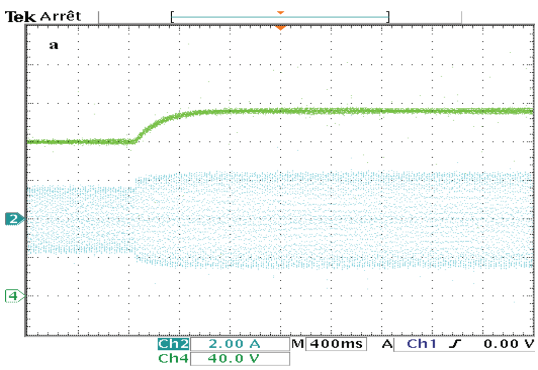

a)

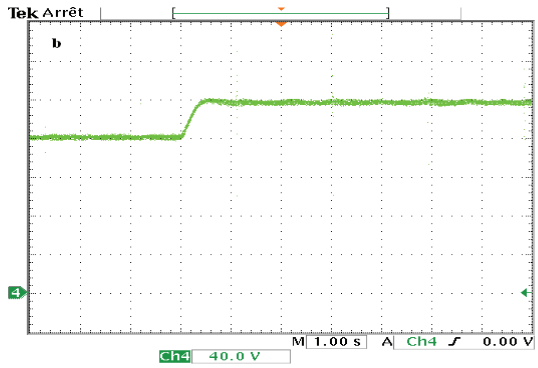

b)

Fig. 12. Transient reference changes: a) PI, b) Fuzzy

It is clear, from these figures that the transient response in the dc-bus voltage is faster with the fuzzy control scheme.

Conclusions

The main goal of the control system is to maintain the dc-bus voltage at the required level, using conventional PI controller or fuzzy logic controller in the dc-bus voltage control loop, while input currents drawn from the power supply should be sinusoidal and in phase with respective phase voltages to satisfy the unity power factor (UPF) operation of the converter. The proposed variable band hysteresis controller, different to the conventional fixed band hysteresis controller, is synthesized by analyzing the instantaneous inductance current. The proposed VBH was simulated and implemented in real-time for both conventional PI and fuzzy logic controller. The presented results indicate that the VBH is much better than the classical one in steady and transient states (dc-bus voltage error =1V, THD of line currents = 2,10%). Near unit power factor can be achieved. Moreover, fuzzy logic controller gives excellent performance in transient state, a good rejection of impact load disturbance, and a good robustness.

References

1. **Henry S. H. C., Eugene P. W. T., Hui S. Y. R.** Development of a Fuzzy Logic Controller for Boost Rectifier with Active Power Factor Correction // IEEE, 1999. – P. 149–154.
2. **Jee–Woo L., Bong–Hwan K.** A Power–Factor Controller for Single Phase PWM Rectifier // IEEE Transaction on Industrial Electronics, 1999. – Vol. 46. – No. 5. – P. 1035–1037.
3. **Jankovskis J., Stepins D., Pikulins D.** Lowering of EMI Noise in Boost Type PFC by the use of Spread Spectrum // Electronics and Electrical Engineering. – Kaunas: Technologija, 2009. – No. 6(94). – P. 15–18.
4. **Masashi O., Hirofumi M.** An AC/DC Converter with High Power Factor // IEEE Transaction on Industrial Electronics, 2003. – Vol. 50. – No. 2. – P. 356–361.
5. **Khoshooei A., Moghani S.** Implementation of a Single Input Fuzzy Controller for a High Power Factor Boost Converter //, 7th Africon conference in Africa, Technology innovation. – IEEE, Gaborone, Botswana, 2004. – P. 69–72.
6. **Sulcius V., Gelezevicius A.** Implementation of the Control Algorithm of the Variable Structure Controller in the Electromechanical Servo System // Electronics and Electrical

Engineering. – Kaunas: Technologija, 2006. – No. 7(71). – P. 51–54.
7. **Diego G. L., Arturo F., Manuel A.** A Unity Power Factor Correction Pre–regulator With Fast Dynamic Response Based on a Low–Cost Microcontroller // IEEE Transaction on Power Electronics, 2008. – Vol. 23. – No. 2. – P. 635–641.
8. **Martin K. H. C., Martin H. L. C., Chi K. T.** Practical Design And Evaluation of A 1 KW PFC Power Supply Based en Reduced Redundant Power Processing Principle // IEEE Transaction on Industrial Electronics, 2008. – Vol. 55. – No. 2. – P. 665–673.
9. **Vishnu M. R., Amit K. J., Kishore K. R., Aman B.** Experimental Comparison of Digital Implementation of Single–Phase PFC Controllers // IEEE Transaction on Industrial Electronics, 2008. – Vol. 55. – No. 1. – P. 67–78.
10. **Belhouchet N., Rahmani L.**, Development of Adaptative Hysteresis–band Current Control of PWM Three–Phase AC Chopper with Constant Switching Frequency // Electric Power Components and systems. – Taylor & Francis, 2009. – Vol. 37. – P. 583–598.

Received 2011 04 02
Accepted after revision 2011 09 08

A. Kessal, L. Rahmani, M. Mostefai, J. Gaubert. Power Factor Correction based on Fuzzy Logic Controller with Fixed Switching Frequency // Electronics and Electrical Engineering. – Kaunas: Technologija, 2012. – No. 2(118). – P. 67–72.

This paper presents an application of different methods to regulate the output voltage of AC-DC converter associated with power factor corrector (PFC), a classical PI regulator was used, and another based on fuzzy logic was built, the both regulators were inserted in the voltage loop. To reduce the total harmonic distortion of the input current to give it a sinusoidal shape, hysteresis bands control were used, the variable band hysteresis give better results compared to other bands. All these controllers have been verified via simulation in Simulink and experimental test. The fuzzy logic inference based controller can achieve better dynamic response than its PI counterpart under large load disturbance and plant uncertainties. Furthermore, the variable hysteresis band control in the current loop gives a low THD of the input current compared to classical bands control. Ill. 12, bibl. 10, tabl. 2 (in English; abstracts in English and Lithuanian).

A. Kessal, L. Rahmani, M. Mostefai, J. Gaubert. Galios koeficiento korekcija, pagrįsta neraiškiosios logikos valdikliu esant fiksuotam perjungimo dažniui // Elektronika ir elektrotechnika. – Kaunas: Technologija, 2012. – Nr. 2(118). – P. 67–72.

Pristatomas skirtingų metodų taikymas AC-DC konverterio su galios koeficiento reguliatoriumi išėjimo įtampai reguliuoti. Klasikinis PI ir neraiškiosios logikos reguliatoriai buvo panaudoti įtampos kilpoje. Siekiant sumažinti harmoninius įėjimo srovės iškraipymus, buvo naudojama histerezės juostų kontrolė. Kintamos juostos histerezės rezultatai būna geresni nei kitų juostų. Visi šie valdikliai buvo patikrinti „Simulink" modeliavimu ir eksperimentiškai. Neraiškiosios logikos valdiklis gali pasiekti geresnes dinamines charakteristikas nei PI valdiklis esant dideliems trikdžiams ir jėgainės neapibrėžtumams. Be to, kintamų histerezės juostų kontrolė srovės kilpoje sukelia nedaug harmoninių iškraipymų, palyginti su klasikine juostų kontrole. Il. 12, bibl. 10, lent. 2 (anglų kalba; santraukos anglų ir lietuvių k.).